PHYSICAL REVIEW A

GENERAL PHYSICS

THIRD SERIES, VOL. 4, NO. 1 JULY 1971

Theoretical L_2- and L_3-Subshell Fluorescence Yields and L_2-L_3X Coster-Kronig Transition Probabilities*

Mau Hsiung Chen and Bernd Crasemann
Department of Physics, University of Oregon, Eugene, Oregon 97403

and

Vaclav O. Kostroun
Ward Reactor Laboratory, Department of Applied Physics, Cornell University, Ithaca, New York 14850
(Received 25 January 1971)

L_2-subshell fluorescence yields ω_2 and L_2-L_3X Coster-Kronig transition probabilities f_{23} have been calculated for 21 elements with atomic numbers $26 \leq Z \leq 93$, and L_3 fluorescence yields ω_3 were computed for 14 atoms with $26 \leq Z \leq 85$. Radiationless transition probabilities were calculated in j-j coupling from screened nonrelativistic hydrogenic wave functions. All contributing Auger matrix elements including states through $4f_{7/2}$ were included. The theoretical Auger widths were combined with Scofield's x-ray emission rates to derive fluorescence yields. Results from ω_2 and ω_3 are in very good agreement with experiment. The calculated Coster-Kronig transition probabilities are close to those derived by McGuire from a self-consistent-field potential. However, the theoretical f_{23} curves differ by $\sim 35\%$ from measured values of f_{23}. No explanation for this discrepancy has been found.

I. INTRODUCTION

The fluorescence yield of an atomic excited state is the relative probability of radiative deexcitation of the state, or the ratio of radiative width to total width of the state. Fluorescence yields are of considerable importance in the interpretation of a wide range of experiments in nuclear and atomic physics. Recent advances in experimental techniques have led to increasingly precise measurements of fluorescence yields of atoms with vacancies in the K, L, and even M shells. A comprehensive review of the subject is in preparation.[1] The growing number of accurate experimental results provides new incentive for efforts to derive fluorescence yields from theory.

In a previous paper,[2] we have shown that atomic K-shell fluorescence yields can be calculated with rather surprising accuracy from Auger matrix elements based on simple nonrelativistic screened hydrogenic wave functions, provided that (a) all radiationless transitions that contribute measurably to the Auger width of a state are meticulously included, (b) careful attention is paid to screening, particularly of the continuum wave function, and (c) radiative widths are derived from relativistic calculations,[3] since they dominate the K-shell width at high Z. In the present article, we report extension of this work to atomic states characterized by a vacancy in the $2p_{1/2}$ or $2p_{3/2}$ subshell.

The definition of L-shell fluorescence yields is complicated by the effect of Coster-Kronig transitions that shift vacancies to higher L subshells. Thus, the vacancy distribution filled through radiative transitions from higher shells is, generally, different from the primary vacancy distribution. The reader is referred to review articles[1,4] for thorough discussions of the pertinent definitions. In the present work, we calculate three basic quantities: (i) the L_3-subshell fluorescence yield $\omega_3 = \Gamma_R^3/\Gamma^3$, defined as the ratio of radiative width Γ_R^3 to total width Γ^3 of an atomic state characterized by a $2p_{3/2}$ hole; (ii) the L_2-subshell fluorescence yield $\omega_2 = \Gamma_R^2/\Gamma^2$, where the total L_2 width

Copyright © 1971 by The American Physical Society.

$\Gamma^2 = \Gamma_R^2 + \Gamma_A^2 + \Gamma^{23}$ is the sum of radiative, Auger, and Coster-Kronig partial widths; and (iii) a_{23}, the radiationless part of the Coster-Kronig transition probability f_{23} of shifting a $2p_{1/2}$ vacancy to the $2p_{3/2}$ subshell. It is generally true[5] that the radiative component ω_{23} of the Coster-Kronig transition probability f_{23} is negligible, whence $a_{23} \cong f_{23}$.

For ease of comparison with experimental results, we also list a derived quantity $\nu_2 \equiv \omega_2 + f_{23}\omega_3$, which is the total yield of L x rays emitted in the deexcitation of an atom with a primary L_2 vacancy.

We omit calculations of quantities pertaining to $2s$-hole states for the following reason: The most intense L_1 Auger transitions are of very low energy, so that large transition-energy uncertainties result from incomplete knowledge of electron binding energies in atoms that are singly or doubly ionized in inner shells. The radiationless transition probabilities depend strongly on the continuum-electron energy. Furthermore, many particular transitions are only energetically possible over restricted ranges of atomic numbers; there is insufficient information on the exact limits of these ranges. It therefore appears that calculations of ω_1 and related Coster-Kronig probabilities are bound to involve large uncertainties until more accurate input data become available.

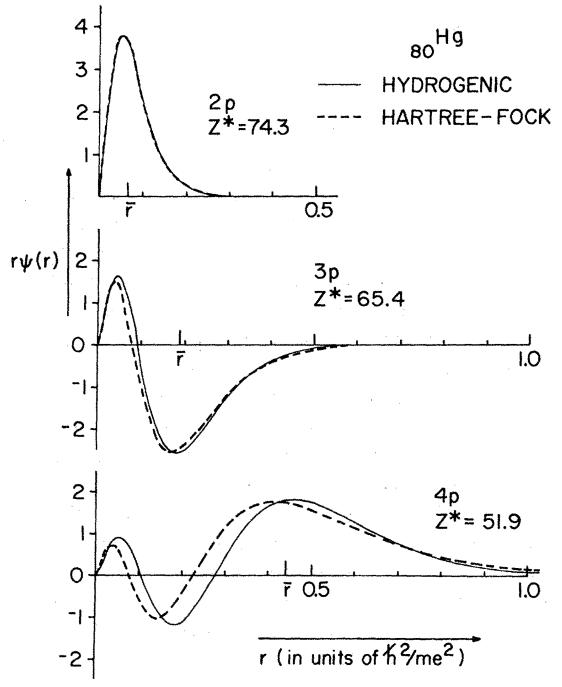

FIG. 1. Comparison of some typical Slater-screened hydrogenic radial wave functions for Hg, as used in the present calculation, with the corresponding SCF wave functions of Mann (Ref. 7).

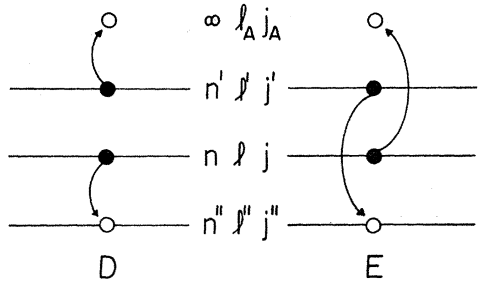

FIG. 2. Schematic representation of direct (D) and exchange (E) radiationless transitions, illustrating the notation used here to designate quantum numbers that characterize the pertinent states.

II. THEORY

The calculation of radiationless transition probabilities is based on Wentzel's *ansatz*.[6] A hole representing the initial atomic vacancy and a hole in the continuum, each described by single-particle wave functions and coupled to a given total angular momentum, undergo a transition due to the Coulomb interaction; the final state consists of two vacancies in bound levels, coupled to the same total angular momentum as in the initial state. Spherical symmetry of the potential is assumed, permitting separation of radial and angular parts of the single-particle wave functions. Screened nonrelativistic hydrogenic wave functions are employed. Neglect of relativistic corrections is not expected to introduce an appreciable error. The use of the analytic hydrogenic wave functions greatly simplifies the calculation. For low principal quantum numbers, these wave functions are quite good at intermediate distances from the nucleus, where the largest contribution to the Auger matrix element is located. This fact is illustrated in Fig. 1, which contains a comparison of some typical screened hydrogenic and Hartree-Fock[7] radial wave functions for Hg. Only in higher shells, an appreciable shift in the position of radial nodes is noted that could lead to errors in the overlap with the continuum wave function. However, if the Coulomb continuum wave function[8] is suitably screened,[2] such errors are minimized.

Bound-state wave functions were screened according to the Hartree recipe,[9] choosing the effective charge Z^* so that the mean hydrogenic radial distance $\langle r \rangle$ coincides with $\langle r \rangle$ as computed from the neutral-atom Hartree-Fock wave functions of Froese.[10] The continuum wave functions were screened in accordance with the procedure developed for the calculation of radiationless transitions to the K shell,[2] whereby Z^* is taken to be the geometric mean of the effective charge appropriate for the state from which the continuum

TABLE I. Theoretical L_i-subshell radiationless widths Γ_A^i, total widths Γ^i, fluorescence yields ω_i, L_2-L_3X partial Coster-Kronig widths Γ_A^{23}, transition probabilities f_{23}, and x-ray yields ν_2.

Element	Γ_A^2 (eV)	Γ^2 (eV)	ω_2	Γ_A^3 (eV)	Γ^3 (eV)	ω_3	Γ_A^{23} (eV)	f_{23}	ν_2
$_{26}$Fe	1.292	1.395	0.001 43	1.321	1.323	0.001 49	0.101	0.0724	0.001 54
$_{28}$Ni	1.324	1.475	0.002 69				0.147	0.0997	
$_{29}$Cu	1.366	1.539	0.003 57	1.401	1.406	0.003 83	0.168	0.109	0.003 99
$_{32}$Ge	1.429	1.477	0.007 72				0.0368	0.0249	
$_{33}$As	1.514	1.594	0.008 85	1.565	1.579	0.008 74	0.0659	0.0413	0.009 21
$_{34}$Se	1.610	1.730	0.009 94				0.103	0.0595	
$_{35}$Br	1.733	1.899	0.010 9				0.145	0.0764	
$_{36}$Kr	1.866	2.083	0.011 9	1.941	1.965	0.012 3	0.192	0.0922	0.013 0
$_{37}$Rb	1.955	2.221	0.013 2				0.237	0.107	
$_{40}$Zr	2.138	2.491	0.018 9	2.238	2.284	0.020 1	0.305	0.123	0.021 4
$_{42}$Mo	2.210	2.603	0.024 5	2.312	2.374	0.025 9	0.329	0.126	0.027 8
$_{47}$Ag	2.406	2.910	0.043 0	2.552	2.672	0.044 9	0.379	0.130	0.048 8
$_{50}$Sn	2.546	3.155	0.056 7				0.430	0.136	
$_{51}$Sb	2.600	3.247	0.061 6	2.798	2.987	0.063 3	0.447	0.138	0.070 3
$_{56}$Ba	2.791	3.682	0.090 7	3.168	3.481	0.089 9	0.557	0.151	0.104
$_{60}$Nd	2.963	4.012	0.120	3.268	3.713	0.120	0.569	0.142	0.137
$_{65}$Tb	3.069	4.363	0.166	3.471	4.133	0.160	0.571	0.131	0.187
$_{74}$W	3.152	5.151	0.271	3.680	4.924	0.253	0.602	0.117	0.301
$_{80}$Hg	3.209	5.942	0.352	3.857	5.683	0.321	0.639	0.108	0.387
$_{85}$At	3.242	6.779	0.422	4.008	6.460	0.380	0.676	0.100	0.460
$_{93}$Np	3.252	9.842	0.460	4.217	7.991	0.472	2.059	0.209	0.559

electron originates and the effective charge pertaining to the next higher state. This approach takes account of the fact that the continuum electron, as it moves away from the nucleus, sees a steadily decreasing charge.

A general analytic expression for the complete radial Auger matrix elements is derived in Ref. 2, to which the reader is referred for details. The

TABLE II. Experimental L_2- and L_3-subshell fluorescence yields ω_2 and ω_3, L_2-L_3X Coster-Kronig transition probabilities f_{23}, and L x-ray yields $\nu_2 = \omega_2 + f_{23}\omega_3$.

Element	ω_2	ω_3	f_{23}	ν_2	Ref.
$_{65}$Tb	0.160 ± 0.018	0.188 ± 0.016	0.090 ± 0.014	0.177 ± 0.019	15
$_{70}$Yb	0.182 ± 0.011	0.183 ± 0.011	0.170 ± 0.009		16
$_{71}$Lu		0.251 ± 0.035		0.290 ± 0.040	17
$_{72}$Hf		0.228 ± 0.025		0.329 ± 0.035	17
$_{73}$Ta		0.254 ± 0.025		0.303 ± 0.030	17
	0.250 ± 0.013	0.228 ± 0.013	0.180 ± 0.007		18
	0.25 ± 0.02	0.27 ± 0.01	0.20 ± 0.04	0.31 ± 0.01	19
$_{74}$W		0.272 ± 0.037		0.330 ± 0.045	17
$_{75}$Re		0.284 ± 0.043		0.347 ± 0.052	17
$_{76}$Os		0.290 ± 0.030		0.366 ± 0.038	17
$_{77}$Ir		0.262 ± 0.036		0.351 ± 0.048	17
$_{78}$Pt		0.317 ± 0.029		0.382 ± 0.035	17
$_{79}$Au		0.317 ± 0.025		0.395 ± 0.032	17
$_{80}$Hg		0.367 ± 0.056		0.455 ± 0.062	17
	0.316 ± 0.010	0.300 ± 0.010	0.190 ± 0.010		21
$_{81}$Tl		0.386 ± 0.053		0.450 ± 0.061	17
	0.319 ± 0.010	0.306 ± 0.010	0.169 ± 0.010	0.371 ± 0.010	22
$_{82}$Pb		0.354 ± 0.028		0.410 ± 0.039	17
	0.363 ± 0.015	0.315 ± 0.013	0.164 ± 0.016	0.417 ± 0.015	20
$_{83}$Bi		0.362 ± 0.029		0.427 ± 0.034	17
	0.23 ± 0.02	0.345 ± 0.018			23
$_{90}$Th		0.517 ± 0.042		0.540 ± 0.043	17
$_{92}$U		0.500 ± 0.040		0.610 ± 0.049	17

angular factors in the Auger matrix elements were computed in j-j coupling. While the total radiationless transition rate is independent of the coupling,[2,11] difficulties arise with the use of LS coupling when the initial vacancy is included in the final configuration,[2] making the j-j scheme most appropriate for the present purpose. All energetically possible transitions that involve electrons through the $4f_{7/2}$ sublevel were included. Thus, to compute the radiationless transition probability for filling an L_3 vacancy in an atom of high atomic number, 1392 direct and an equal number of exchange matrix elements were computed; for an initial L_2 vacancy, the number of direct and exchange matrix elements included in the calculation was 178 each for high Z.

Electron binding energies used in these calculations were taken from the compilation of Bearden and Burr.[12] Following Callan,[8,13] we used neutral-atom binding energies for $E_{n''l''j''}$ and E_{n1j} (see Fig. 2 for notation). To take account of decreased screening due to inner-shell ionization, the binding energy of a neutral atom of the next higher atomic number $Z+1$ was taken for $E_{n'l'j'}$.

Radiationless transition probabilities computed in the manner outlined above were combined with x-ray emission rates calculated by Scofield[3,14] from relativisitic Hartree-Fock-Slater wave functions, in order to find fluorescence yields.

III. RESULTS AND DISCUSSION

A. L_2-Subshell Fluorescence Yields

Our calculated L_2 radiationless widths Γ_A^2 are listed in Table I for selected elements from Fe through Np, together with total L_2-level widths Γ^2 obtained by adding Scofield's[3,14] radiative widths and our calculated Coster-Kronig widths Γ_A^{23} to Γ_A^2. The fourth column in Table I contains the theoretical L_2 fluorescence yields ω_2 derived from these widths.

Experimental information for comparison with these results is still relatively scarce. Measurements of pertinent quantities[15-23] are summarized in Table II. There are no direct measurements of ω_2 below $Z=65$. However, empirical L_2-level widths can be derived from x-ray emission linewidths. For elements from $_{37}$Rb through $_{50}$Sn, Gokhale[24] has measured $K\alpha_2$ linewidths. Subtracting total K-level widths derived by Leisi *et al.*[25] from the x-ray linewidth measurements of various authors, total L_2 widths are found that can be combined with Scofield's[3,14] theoretical L_2 radiative widths to derive values of ω_2, as indicated in Table III. All this empirical and semiempirical information on ω_2 is compared in Fig. 3 with our theoretical curve and with the recent theoretical results of McGuire.[26] This latter author used wave functions calculated in a very different manner. He computed the quantity $-rV(r)$ by the self-consistent-field (SCF) approach of Herman and Skillman,[27] made a piecewise straight-line approximation to the potential function, and hence obtained a one-electron Schrödinger equation that he could solve exactly in terms of Whittaker functions for the radial part. From these solutions, he calculated both radiative and radiationless transition rates.

B. L_3-Subshell Fluorescence Yields

Theoretical L_3 radiationless and total widths and fluorescence yields are listed in Table I for a number of elements with $26 \leq Z \leq 85$. The cost of com-

TABLE III. L_2- and L_3-subshell fluorescence yields ω_2 and ω_3, derived from the semiempirical K-level widths Γ^K of Leisi *et al.* (see Ref. 25), x-ray emission linewidths $\Gamma(K\alpha_2)$ and $\Gamma(K\alpha_1)$ measured by Gokhale (see Ref. 24), and Scofield's (see Refs. 3 and 14) theoretical L_2 and L_3 radiative widths Γ_R^2 and Γ_R^3. Total L_2- and L_3-level widths Γ^2 and Γ^3 are also listed.

Element	Γ^K (eV)	$\Gamma(K\alpha_2)$ (eV)	Γ^2 (eV)	Γ_R^2 (eV)	ω_2	$\Gamma(K\alpha_1)$ (eV)	Γ^3 (eV)	Γ_R^3 (eV)	ω_3
$_{37}$Rb	2.518	4.79	2.272	0.029 29	0.0129	4.39	1.872	0.028 50	0.0152
$_{38}$Sr	2.796	4.79	1.994	0.034 47	0.0173	4.83	2.034	0.033 49	0.0165
$_{39}$Y	3.097	5.16	2.063	0.040 46	0.0196	5.10	2.003	0.039 26	0.0196
$_{40}$Zr	3.421	5.93	2.509	0.047 26	0.0188	5.49	2.069	0.045 79	0.0221
$_{41}$Nb	3.770	6.02	2.250	0.055 14	0.0245	5.97	2.200	0.053 31	0.0242
$_{42}$Mo	4.144	6.66	2.516	0.063 84	0.0254	6.42	2.276	0.061 61	0.0271
$_{44}$Ru	4.975	7.32	2.345	0.084 52	0.0360	7.15	2.175	0.081 25	0.0374
$_{45}$Rh	5.435	7.91	2.475	0.096 70	0.0391	7.86	2.425	0.092 76	0.0383
$_{46}$Pd	5.925	8.39	2.465	0.110 5	0.0448	8.44	2.515	0.105 7	0.0420
$_{47}$Ag	6.447	9.38	2.933	0.125 3	0.0427	9.09	2.643	0.119 6	0.0453
$_{48}$Cd	7.004	10.03	3.026	0.141 5	0.0468	9.98	2.976	0.134 9	0.0453
$_{49}$In	7.595	10.75	3.155	0.159 3	0.0505	10.42	2.825	0.151 5	0.0536
$_{50}$Sn	8.222	12.27	4.048	0.178 6	0.0441	11.15	2.928	0.169 6	0.0579

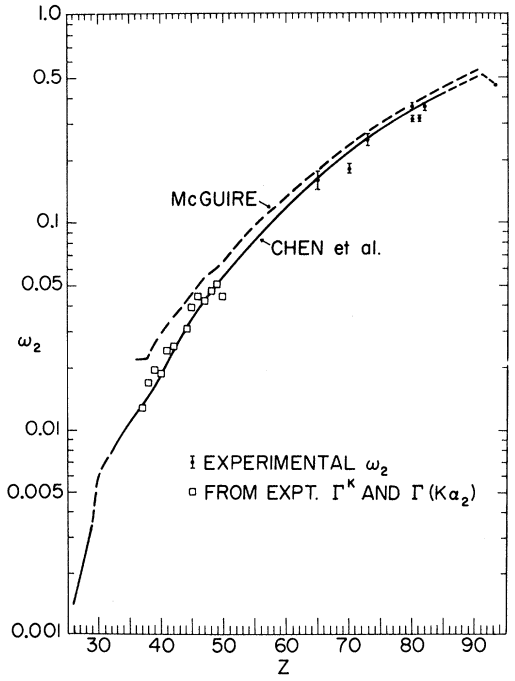

FIG. 3. L_2-subshell fluorescence yield ω_2 as a function of atomic number. The solid curve links results of the present calculation (Table I); the dashed curve represents the results of a calculation by McGuire, based on an SCF potential (Ref. 26). Experimental points for $Z \geq 65$ are those listed in Table II; semiempirical points were derived from measured x-ray emission linewidths as discussed in Sec. III A (see Table III). The fluorescence yield ω_2 increases abruptly at $Z \cong 31$, where L_2-$L_3M_{4,5}$ Coster-Kronig transitions become energetically impossible, and drops sharply at $Z \cong 91$, where transitions of the L_2-L_3M_5 type again become possible (see Sec. III C).

puting up to 2784 Auger matrix elements per atom made it necessary to limit these calculations to 14 representative elements.

Figure 4 contains a comparison of our and McGuire's[26] theoretical ω_3 curves with measured values from Table II and semiempirical L_3 fluorescence yields derived from Gokhale's[24] $K\alpha_1$ linewidth measurements, the empirical K-level widths of Leisi *et al.*,[25] and Scofield's[3,14] theoretical x-ray emission rates (see Table III).

C. L_2-L_3X Coster-Kronig Transition Probabilities

An L_2 vacancy can switch to the L_3 subshell before being filled through a transition from another major shell. Such transitions between subshells are named after Coster and Kronig, who discovered them through the study of x-ray satellite lines.[28] Coster-Kronig transition probabilities play an important role in a self-consistent scheme of defining subshell fluorescence yields.[1,4] The partial L_2-level widths Γ_A^{23} due to radiationless transitions of the L_2-L_3X type, computed in the present work, are included in Table I. The corresponding Coster-Kronig transition probabilities f_{23} are also listed; these have been computed on the assumption that radiative L_2-L_3 transitions can be neglected, being of magnetic-dipole (spin-flip) character. Theoretical and experimental evidence confirming this assumption has recently been gained.[5]

A curve linking our calculated values of f_{23} is shown in Fig. 5. A sharp discontinuity occurs at $Z \cong 30$; above this atomic number, the intense L_2-$L_3M_{4,5}$ radiationless transitions become energetically impossible, since the $M_{4,5}$ binding energy in an L_2-ionized atom exceeds the $2p_{1/2}$-$2p_{3/2}$ spin-orbit coupling energy difference. A sharp rise in f_{23} takes place at $Z \cong 91$; at higher atomic numbers, L_2-L_3M_5 Auger transitions are again possible.

Also shown in Fig. 5 are values of f_{23} computed by McGuire[26] from an SCF potential as indicated in Sec. III A. The very close agreement of McGuire's and our results (except for $47 \leq Z \leq 54$) is especially gratifying in view of the drastically different approaches used in the two calculations. All the more perplexing is the disagreement with experiment. Of seven experimental results (see

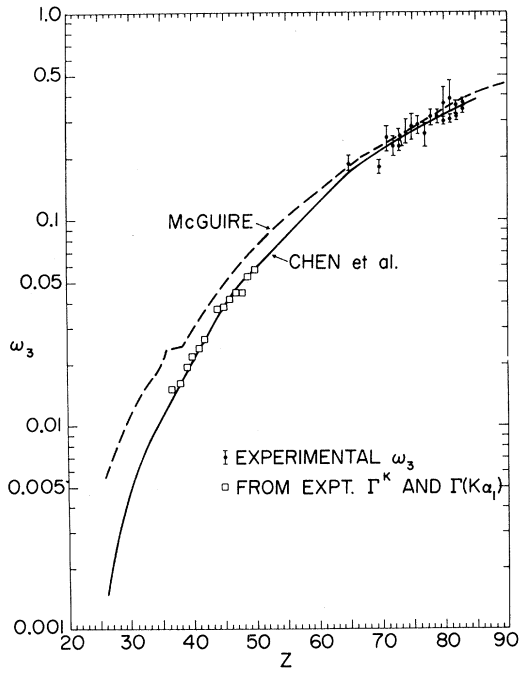

FIG. 4. L_3-subshell fluorescence yield ω_3 as a function of atomic number. Results of the present calculation (solid curve) are compared with the SCF-potential calculation of McGuire (Ref. 26), experimental points (Table II), and semiempirical results derived from measured x-ray linewidths (Table III).

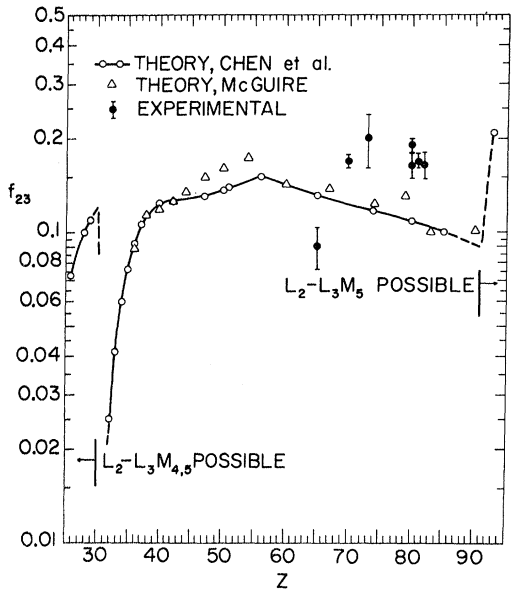

FIG. 5. Theoretical L_2-L_3X Coster-Kronig transition probability f_{23} from the present work (solid curve), compared with the results of McGuire (Ref. 26) and with experimental points (Table II). Discontinuities in f_{23} occur near $Z=31$, where the prominent transitions of the L_2-$L_3M_{4,5}$ type become energetically impossible, and near $Z=91$, above which atomic number transitions of the L_2-L_3M_5 type are again possible. The poor agreement between theory and experiment remains unexplained.

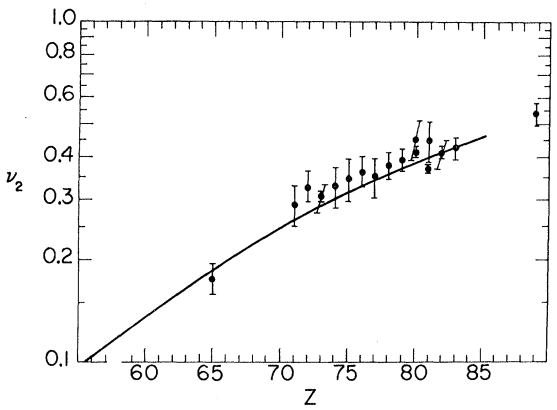

FIG. 6. Theoretical L x-ray yield $\nu_2=\omega_2+f_{23}\omega_3$ (solid curve), compared with experimental data (Table II).

Table II) obtained by an x-ray coincidence technique,[19] the six measurements for $Z \geq 70$ exceed the calculated transition probability, while the single measurement for $Z=65$ lies below the theoretical curve. The discrepancies are of the order of 35% of the experimental results, far in excess of errors of measurement. Radiative Coster-Kronig transitions cannot be invoked to account for more than an infinitesimal part of the difference.[5] The theoretical approach appears to have been proven by the very close agreement of calculated values of ω_2 and ω_3 with experiment, but those subshell fluorescence-yield calculations are less sensitive to the input binding energies than the Coster-Kronig probability calculations. At the present time, the f_{23} discrepancy remains unexplained.

D. X-Ray Yields υ_2

A quantity determined rather directly in many experiments (see Table II) is the total yield ν_2 of L-series x rays emitted in the deexcitation of an atom with a primary L_2 vacancy. This yield

$$\nu_2=\omega_2+f_{23}\omega_3$$

is included in Table I and is compared with experimental results in Fig. 6.

ACKNOWLEDGMENTS

We wish to thank Professor P. Venugopala Rao of Emory University for helpful comments and Dr. J. H. Scofield of the Lawrence Radiation Laboratory, Livermore, for supplying us with unpublished theoretical L x-ray emission rates for certain elements. Dr. E. J. McGuire of the Sandia Laboratories kindly communicated results of some of his calculations to us in advance of publication, and Dr. R. W. Fink of the Georgia Institute of Technology kindly made preprints of recent work by his group available.

*Work supported in part by the U. S. Atomic Energy Commission under Contract No. AT(45-1)-1925.

[1]W. Bambynek, B. Crasemann, R. W. Fink, H. U. Freund, Hans Mark, R. E. Price, P. Venugopala Rao, and C. D. Swift (unpublished).

[2]V. O. Kostroun, M. H. Chen, and B. Crasemann, Phys. Rev. A 3, 533 (1971).

[3]J. H. Scofield, Phys. Rev. 179, 9 (1969).

[4]R. W. Fink, R. C. Jopson, Hans Mark, and C. D. Swift, Rev. Mod. Phys. 38, 513 (1966).

[5]M. H. Chen, B. Crasemann, P. Venugopala Rao, J. M. Palms, and R. E. Wood, Bull. Am. Phys. Soc. 16, 618 (1971); and unpublished.

[6]G. Wentzel, Z. Physik 43, 524 (1927).

[7]J. B. Mann, LASL Report No. LA-3691, 1968 (unpublished).

[8]E. J. Callan, Phys. Rev. 124, 793 (1961).

[9]D. Hartree, *The Calculation of Atomic Structures* (Wiley, New York, 1957), Chap. 7.

[10]C. Froese (unpublished).

[11]R. A. Rubenstein, thesis (University of Illinois, 1955) (unpublished).

[12]J. A. Bearden and A. F. Burr, Rev. Mod. Phys. 39, 125 (1967).
[13]E. J. Callan, in *Role of Atomic Electrons in Nuclear Transformations* (Nuclear Energy Information Center, Warsaw, 1963), Vol. 3, p. 419.
[14]J. H. Scofield (private communication).
[15]J. C. McGeorge, H. U. Freund, and R. W. Fink, Nucl. Phys. A154, 526 (1970).
[16]S. Mohan, H. U. Freund, R. W. Fink, and P. Venugopala Rao, Phys. Rev. C 1, 254 (1970).
[17]R. E. Price, Hans Mark, and C. D. Swift, Phys. Rev. 176, 3 (1968).
[18]S. Mohan, R. W. Fink, R. E. Wood, J. M. Palms, and P. Venugopala Rao, Z. Physik 239, 423 (1970).
[19]P. Venugopala Rao and B. Crasemann, Phys. Rev. 139, A1926 (1965).
[20]P. Venugopala Rao, R. E. Wood, J. M. Palms, and R. W. Fink, Phys. Rev. 178, 1997 (1969).
[21]J. M. Palms, R. E. Wood, P. Venugopala Rao, and V. O. Kostroun, Phys. Rev. C 2, 592 (1970).
[22]R. E. Wood, J. M. Palms, and P. Venugopala Rao, Phys. Rev. 187, 1497 (1969).
[23]H. U. Freund and R. W. Fink, Phys. Rev. 178, 1952 (1969).
[24]B. G. Gokhale, Ann. Phys. (Paris) 7, 852 (1952).
[25]H. J. Leisi, J. H. Brunner, C. F. Perdrisat, and P. Scherrer, Helv. Phys. Acta 34, 161 (1961).
[26]E. J. McGuire, Phys. Rev. A 3, 587 (1971).
[27]F. Herman and S. Skillman, *Atomic Structure Calculations* (Prentice-Hall, Englewood Cliffs, N. J., 1963).
[28]D. Coster and R. de L. Kronig, Physica 2, 13 (1935).

PHYSICAL REVIEW A VOLUME 4, NUMBER 1 JULY 1971

Dynamic Polarizabilities and Refractive Indexes of H^- and Li^+ Ions

Kwong T. Chung
Department of Physics, North Carolina State University, Raleigh, North Carolina 27607
(Received 28 January 1971)

A variational perturbation method is used to evaluate the first-order wave functions of H^- and Li^+ in the presence of a monochromatic electromagnetic field. These functions are utilized to calculate the dynamic polarizabilities and refractive indexes of H^- and Li^+ ions. Converged results are obtained for both systems. The converged static polarizability of H^- in the present calculation is shown to be 206.0 a.u., which compares favorably with previous theoretical calculations. The wavelength for the Li^+ 1^1S-2^1p transition from the dynamic polarizability calculation, 199.16 Å, is compared with the exact theoretical value of 199.32 Å.

INTRODUCTION

The interaction between radiation and matter has been investigated extensively in recent years. Theoretical work has been done using a semiclassical approach. For atomic systems, variational[1] and variational perturbation methods have been constructed.[2] The advantages of these methods are that in the Schrödinger perturbation theory the infinite summation for the first-order wave function is summed over through a variational procedure, thus enabling us to calculate the first-order wave function of the perturbed system accurately. Static and dynamic polarizabilities are readily obtained with excellent agreement with experiment.[1,3] The first-order wave function in a frequency-dependent electric field is particularly interesting because it can also be used to calculate the two-photon processes for atomic systems such as spontaneous emission, photon ionization, and photodetachment.[4] Hence, the purpose of the present work is twofold: first, to generate a set of accurate first-order wave functions for the two-electron systems in the presence of a frequency-dependent electric field, and next, to use these to calculate the dynamic polarizabilities and refractive indexes of Li^+ and H^- ions. In a subsequent work, these functions will be used to investigate two-photon ionization and detachment processes.

For the helium atom, the dynamic polarizability has been calculated accurately by Chan and Dalgarno[3] using a variational perturbation method and by Dutta *et al.*[5] using a many-body technique. The most accurate result for this atom is obtained by Chung[1] using a variational procedure and a 2^1p-type first-order wave function. This type of first-order wave function will again be used in the present work.

For two-electron ions, the available theoretical calculations in the literature are more limited. For the ground state of Li^+, a coupled Hartree-Fock calculation has been applied[6]; besides this, Dalgarno and Victor[7] have also used the imaginary frequency dynamic polarizability to calculate the van der Waals forces between this ion and other atomic systems. To our knowledge, the dynamic polarizability of H^- has not been reported. This is perhaps partly because of the poor convergence of the static polarizability calculations for this ion. In this respect, it is interesting to note a previous work by